ISSN 1672-9145 **Acta Biochimica et Biophysica Sinica** 2005, **37**(9): 634–642 **CN** 31-1940/Q

Study of MMLV RT⁻ Binding with DNA using Surface Plasmon Resonance Biosensor

Lei WU[1], Ming-Hui HUANG[2], Jian-Long ZHAO[1]*, and Meng-Su YANG[1,2]*

[1] *Shanghai Institute of Microsystem and Information Technology, Chinese Academy of Sciences, Shanghai 200050, China*
[2] *Department of Biology and Chemistry, City University of Hong Kong, Hong Kong, China*

Abstract Surface plasmon resonance biosensor technique was used to study the binding of Moloney murine leukemia virus reverse transcriptase without RNase H domain (MMLV RT⁻) with DNA in the absence and in the presence of inhibitors. Different DNA substrates, including single-stranded DNA (ssDNA), DNA template-primer (T-P) duplex and gapped DNA, were immobilized on the biosensor chip surface using streptavidin-biotin, and MMLV RT⁻-DNA binding kinetics were analyzed by different models. MMLV RT⁻ could bind with ssDNA and the binding was involved in conformation change. MMLV RT⁻ binding DNA T-P duplex and gapped DNA could be analyzed using the simple 1:1 Langmuir model. The lack of RNase H domain reduced the affinity between MMLV RT⁻ and T-P duplex. The effects of RT inhibitors, including efavirenz, nevirapine and quercetin, on the interaction between MMLV RT⁻ and gapped DNA were analyzed according to recovered kinetics parameters. Efavirenz slightly interfered with the binding between RT and DNA and the affinity constant in the presence of the inhibitor (K_A=1.21×10^6 M^{-1}) was lower than in the absence of the inhibitor (K_A=4.61×10^6 M^{-1}). Nevirapine induced relatively tight binding between RT and DNA and the affinity constant in the presence of the inhibitor (K_A=1.47×10^7 M^{-1}) was approximately three folds higher than without nevirapine, mainly due to rapid association and slow dissociation. Quercetin, a flavonoid originating from plant which has previously shown strong inhibition of the activity of RT, was found to have minimal effect on the RT-DNA binding.

Key words surface plasmon resonance biosensor; reverse transcriptase; kinetics; inhibitor

Reverse transcriptase (RT) plays an important role in the life of retroviruses. RT possesses ribonuclease H as well as RNA-directed and DNA-directed DNA polymerase activities. It can convert a single-stranded RNA of the retrovirus into a double-stranded DNA for integration into the host genome.

The inhibition of RT polymerase activity is a major treatment method for human immunodeficiency virus type 1 (HIV-1). HIV-1 RT inhibitors are subdivided into nucleoside reverse transcriptase inhibitors (NRTIs) and non-nucleoside reverse transcriptase inhibitors (NNRTIs). NRTIs are the analogs of nucleotides or nucleosides. *In vivo* NRTIs are converted into triphosphate and incorporated into DNA, which blocks the elongation of DNA. NNRTIs are largely hydrophobic inhibitors and do not require intracellular metabolism for activity, so they can be applied directly to study the interaction between RT and its inhibitors. Structural evidence has shown that the allosteric NNRTIs bind tightly to a hydrophobic pocket about 10 Å away from the polymerase site [1–3]. Steady-state kinetic studies suggested the inhibitors were non-competive or uncompetitive with respect to the binding of DNA template-primer (T-P) duplex [4–6]. Although there are many publications on the mechanism of the function of NNRTIs, the kinetics of the interaction between RT and DNA T-P in the presence of NNRTIs has not been well studied. Besides

Received: November 23, 2004 Accepted: June 8, 2005
This work was supported by a grant from the Major Basic Research Program of the Science and Technology Commission Foundation of Shanghai (No. 04JC14081)
*Corresponding authors:
Jian-Long ZHAO: Tel, 86-21-62511070-5709; Fax, 86-21-62511070-8714; E-mail, jianlong_zhao@yahoo.com
Meng-Su YANG: Tel, 852-27887797; Fax, 852-27887406; E-mail, bhmyang@cityu.edu.hk

DOI: 10.1111/j.1745-7270.2005.00088.x

synthesized compounds, natural anti-HIV inhibitors have also been studied by some researchers. *In vitro* experiments showed that several flavonoids, including quercetin, myricetin, baicalein and quercetagenin, were inhibitors of HIV-1 RT and moloney murine leukemia virus RT (MMLV RT) [7–10]. However, it is unclear how these flavonoids act on RT and function as RT inhibitors.

Surface plasmon resonance (SPR) biosensor technique has been proven to be a useful tool for obtaining quantitative kinetic and affinity information on biomolecular interactions. An SPR biosensor can translate a biospecific interaction between a ligand in solution and a binding partner immobilized on the surface into a detectable signal that is directly proportional to the extent of the interaction. The SPR technique offers significant advantages because it is label-free and non-invasive and results are in real time, which contributes significantly to the understanding of the interaction between protein and DNA [11–14].

MMLV RT without RNase H domain (MMLV RT⁻) has been used as a model to investigate RT binding with DNA in the absence and the presence of inhibitors using an SPR biosensor. The elimination of the RNase H domain of MMLV RT does not affect the structural integrity of the polymerase domain [15]. MMLV RT is a monomer with a molecular weight of 75 kDa and has a right-hand structure similar to HIV-1 RT. The fingers and palm domains of MMLV RT resemble those of HIV-1 RT except that there are additional 16 residues at the N-terminal, which relate to the monomer's resistance to proteolytic degradation and dimerization [2]. For both RTs, the active site of polymerase is located at the junction of the fingers and palm domains, which has three highly conserved aspartate residues required for polymerase activity [2]. Because of significant structural homology, the effects of inhibitors on MMLV RT⁻ activity can provide valuable information to develop agents against HIV-1 RT.

In the present study, the binding characteristics of MMLV RT⁻ to various DNA substrates, including single-stranded DNA (ssDNA), DNA T-P duplex and gapped DNA, were determined and compared systematically to establish the binding pattern of RT. Furthermore, the effects of different inhibitors, including two known NNRTIs, efavirenz (EFV) and nevirapine (NVP), and a natural product inhibitor, quercetin, on the binding affinity of MMLV RT⁻ and binding modes with DNA were investigated.

Materials and Methods

Materials

Sensor chip CM5 of research grade, HSB-EP buffer [10 mM HEPES, pH 7.4, 150 mM NaCl, 3 mM EDTA, 0.005% (*V*/*V*) surfactant P20], the amine-coupling kit containing *N*-hydroxysuccinimide (NHS), *N*-ethyl-*N*-(3-diethylaminopropyl)-carbodimide (EDC) and ethanolamine hydrochloride were obtained from Pharmacia Biosensor AB (Uppsala, Sweden). Streptavidin was purchased from Sigma (St. Louis, USA).

MMLV RT⁻ (SuperScript II RT) was purchased from Invitrogen Life Technologies (Carlsbad, USA), and its purity was at least 95% as demonstrated by SDS-PAGE with Coomassie blue staining. The molarity of MMLV RT⁻ was offered by Invitrogen Life Technologies (California, USA).

EFV was generously provided by Bristol-Myers Squibb Company (Princeton, USA) and NVP was a gift from Desano Company (Shanghai, China). Quercetin was purchased from Tauto Biotech Company (Shenzhen, China).

One 5′-biotinylated oligoribo(deoxy)nucleotide and two nonbiotinylated complementary strands (**Table 1**) were synthesized and purified by HPLC (Sangon, Shanghai, China). To facilitate annealing of the oligonucleotides to form duplexes, equimolar amounts of oligonucleotides were mixed together in HSM buffer (10 mM HEPES, pH 7.4, 150 mM NaCl, 10 mM $MgCl_2$). The mixtures were incubated at 99 °C for 5 min and allowed to cool slowly to room temperature. The 15-mer fully annealed to the 50-mer template to form DNA T-P duplex, and the 15-mer

Table 1 Three kinds of DNA substrates

DNA substrate	Sequence
Single-stranded DNA template	5′-biotin-GCATCAACGCACGTTAGCGACTGATACCAAGACTGCCCTTGGACGGCTGC-3′
DNA T-P duplex	5′-biotin-GCATCAACGCACGTTAGCGACTGATACCAAGACTGCCCTTGGACGGCTGC-3′ 3′-GGGAACCTGCCGACG-5′
Gapped DNA	5′-biotin-GCATCAACGCACGTTAGCGACTGATACCAAGACTGCCCTTGGACGGCTGC-3′ 3′-CGTAGTTGCGTGCAATCGCTGACTATG-5′ 3′-GGGAACCTGCCGACG-5′

and 27-mer oligonucleotides fully annealed to the 50-mer template to form gapped DNA with an 8-mer gap in the middle.

Immobilization of DNA substrates on the biosensor chip

The CM5 chip was modified by streptavidin according to the standard protocol (http://www.biacore.com). After the CM5 sensor chip was fully equilibrated by HSB-EP buffer, 35 μl mixture of EDC (0.2 M) and NHS (0.05 M) flowed over the chip surface for 7 min to activate the carboxyl groups on the surface. Then 35 μl streptavidin (200 μg/ml) in 10 mM sodium acetate (pH 4.8) flowed over the chip surface and reacted for 7 min. Finally, 35 μl ethanolamine was used to deactivate the excessive carboxyl groups. After the streptavidin-modified surface was equilibrated with HSM buffer, the DNA solution was injected. The DNA substrates were immobilized on the sensor chip surface by biotin-streptavidin chemistry, with a 5′-biotin-labeled template as the anchor.

Biosensor measurement of the MMLV RT$^-$ binding with DNA

All SPR measurements were carried out using BIAcoreX apparatus (Pharmacia Biosensor AB). The basic principle of the SPR biosensor has been described in detail elsewhere [16].

All binding experiments were carried out at 25 °C with a constant flow of HSM buffer at 5 μl/min. Sensor surface without DNA coating was used as the reference surface. The constant flow ran simultaneously for each binding experiment to minimize variations caused by analyte heterogeneity, non-specific binding and bulk-refractive index changes.

Ten microliters of HSM solution comprising MMLV RT$^-$ at different concentrations was injected over the DNA-modified surface for 120 s, then washed with HSM buffer for 200 s. The DNA-modified surface was regenerated by washing with 10 μl 1% SDS-HSM solution for 1 min to remove protein from the DNA substrates. The successive injection of MMLV RT$^-$ solution was carried out when the baseline reached a level approximate to that before the previous injection.

Biosensor measurement of MMLV RT$^-$ binding with DNA in the presence of different inhibitors

EFV, NVP and quercetin have poor solubility in aqueous buffer, so stock solutions of these potent inhibitors were prepared in dimethyl sulfoxide (DMSO), all at a concentration of 100 mM. The stock solutions were diluted by HSM buffer to a final concentration of less than 100 μM in all experiments, containing less than 0.1% DMSO in the analyte solution.

To study the nature of MMLV RT$^-$ binding with the gapped DNA in the drug solution, MMLV RT$^-$ was fully mixed with a certain inhibitor at a constant concentration. The inhibitor in appropriate concentration, which was determined to be 50 μM, can induce a distinct response comparable to the response induced by the free RT binding with DNA, and will not increase the non-specific adsorption of MMLV RT$^-$ with reference surface. The mixtures were injected over the gapped DNA modified surface for 120 s, then washed with HSM buffer for 200 s.

Because the concentration of each inhibitor (50 μM) in the solution was more than 250-fold in excess of MMLV RT$^-$, and NNRTIs can tightly bind with RT [3], RT was assumed to be saturated with the compound and the concentration of free enzymes could be omitted before the mixture was injected.

Kinetics and data analysis

All experiment data were analyzed using BIAevaluation software (version 4.1; Pharmacia Biosensor AB). The numerical integration algorithms used by BIAevaluation software are sensitive to the sets of parameters and may deviate from the true kinetics. Direct and global curve fitting is an optimum approach for data analysis corresponding to the different possible models. It can avoid deviation caused by limitation of the mass transport from the bulk solution to the sensor surface or inhomogeneity of the binding sites [17]. Therefore all kinetic analyses were performed by global curve fitting. Kinetic parameters of the binding interactions were derived from the response curves by non-linear curve fitting with various possible kinetic models. The degree of randomness of the residual plot and the reduced χ^2 value were used to assess the appropriateness of the various models for analysis of the biosensor data. In all data fittings, we considered the baseline drift. The value of the drift was less than 0.05 response units (RU)/s in all the experiments, so the drift could not cause significant deviation.

Results

The stability of modified surfaces and specificity of MMLV RT$^-$ binding

Schematic representations of the different DNA substrates captured on the streptavidin-modified surface

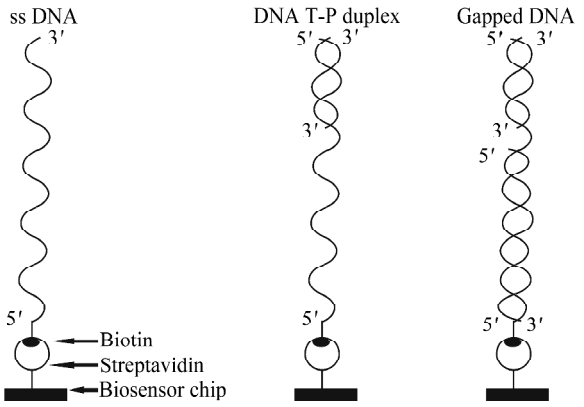

Fig. 1 Schematic representations of the different DNA substrates captured on the streptavidin-modified surface

ssDNA, single-stranded DNA; T-P, template-primer.

are shown in **Fig. 1**. Approximately 1.4×10^{-14} mol/mm^2 of streptavidin and 3.0×10^{-14} mol/mm^2 of DNA substrate were immobilized on the sensor chip surface according to the calculation using the difference in the response levels before and after immobilization, where 1000 RU corresponds to a surface density of approximately 1 ng protein (or 0.8 ng DNA) per square millimeter. Each immobilized streptavidin molecule can bind with about two DNA molecules. No distinct change of response level was observed after a typical experiment, so the surface immobilized with DNA could be used repeatedly.

The specificity of MMLV RT⁻ binding with DNA was tested by comparing the response level curves on the streptavidin-modified surface before and after DNA immobilization. The representative experiment data are shown in **Fig. 2**. Weak binding between MMLV RT⁻ and the streptavidin-modified surface was observed which represented negligible non-specific adsorption. Distinct non-linear association and dissociation were observed when MMLV RT⁻ flowed over the DNA-modified surface. With 120 nM MMLV RT⁻ interacting with the surfaces, about 330 RU was obtained at the end of association after the response data on the streptavidin-coated surface were subtracted from those obtained on the DNA-coated surface (**Fig. 2**), which verified the specificity of MMLV RT⁻-DNA binding.

MMLV RT⁻ binding with different DNA substrates immobilized on the sensor chips

The interactions between MMLV RT⁻ at different concentrations and the immobilized DNA substrates were measured in real time (**Figs. 3–5**). The overall sensor responses increased as time went on and as the concentration of RT increased.

Previous mechanistic studies suggested a three-step binding model of T-P duplex with RT including an initial binding phase and two subsequent conformation change phases [4,18]. Footprint analysis showed MMLV RT⁻ protected the part of the T-P duplex as far as position –15

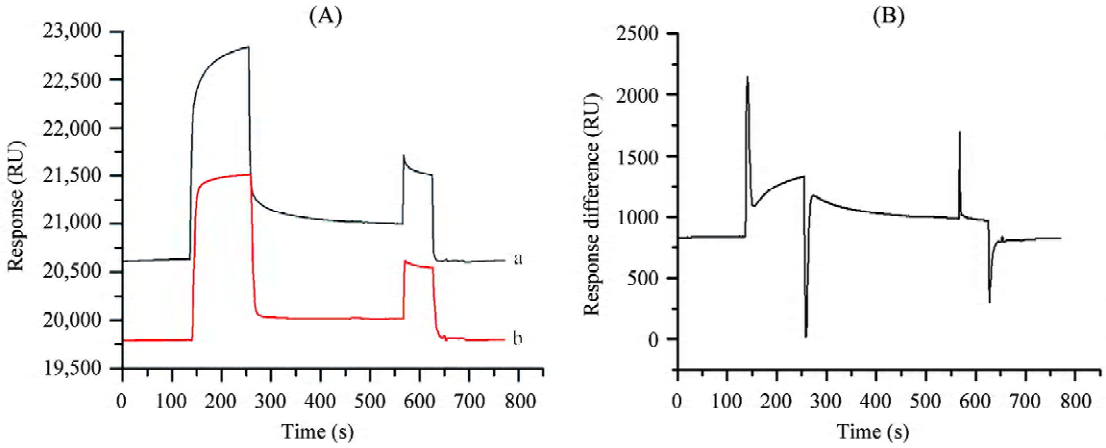

Fig. 2 Specificity of MMLV RT⁻ binding

(A) Curves a and b represent the responses on the streptavidin-modified surface and the gapped DNA-modified surface, respectively, when 120 nM MMLV RT⁻ in HSM buffer flowed over these surfaces sequentially at the flow rate of 5 μl/min at 25 ℃ from 145 s to 265 s. After RT solution was injected, HSM flowed over the surfaces and the dissociation data were recorded for 200 s. Then 10 μl 0.5% SDS-HSM buffer was injected from 580 s to 640 s to regenerate the surface. The responses of the surfaces almost returned to previous levels after regeneration, which showed this method was effective and sufficient. (B) Curve a subtracted from curve b. The spikes were due to the small time difference in the enzyme solution reaching the two different surfaces. RU, response unit.

and the template as far as position +6 [15]. The DNA T-P duplex including an overhang single template part (35-mer) and the gapped DNA including a duplex part (27 bp) in the vicinity of the biosensor chip surface might provide the second RT binding site as well as the DNA T-P part away from the surface. Therefore, the 1:1 Langmuir model (**Equation 1**), the conformation change model (**Equation 2**) and the parallel reaction model (**Equation 3**) were used

$$E+D \underset{k_d}{\overset{k_a}{\rightleftharpoons}} ED, \quad K_A=\frac{k_a}{k_d} \tag{1}$$

$$E+D \underset{k_{d1}}{\overset{k_{a1}}{\rightleftharpoons}} ED, \quad E+D \underset{k_{d2}}{\overset{k_{a2}}{\rightleftharpoons}} (ED)x,$$

$$K_A=\frac{k_{a1}}{k_{d1}}\left(1+\frac{k_{a2}}{k_{d2}}\right) \tag{2}$$

$$E+D \underset{k_{d1}}{\overset{k_{a1}}{\rightleftharpoons}} ED1, \quad K_A=\frac{k_{a1}}{k_{d1}};$$

$$E+D \underset{k_{d2}}{\overset{k_{a2}}{\rightleftharpoons}} ED2, \quad K_A=\frac{k_{a2}}{k_{d2}} \tag{3}$$

to fit the response curves of MMLV RT$^-$ binding with the different DNA substrates, where E and D represent MMLV RT$^-$ in solution and DNA immobilized on the biosensor chip, respectively, and (ED)x represents a complex in another conformation different from the ED complex. The corresponding residual plots are shown in **Figs. 3–5**.

The conformation change model was appropriate to represent the MMLV RT$^-$ binding with the ssDNA due to the small χ^2 value and random residual distribution (**Fig. 3**). When fitting the response curves of MMLV RT$^-$ binding with the DNA T-P duplex or the gapped DNA, the χ^2 value and residual randomness were acceptable for all three models (**Figs. 4** and **5**). However, the conformation change model and the parallel reaction model could not improve the degree of randomness of the residual plots and reduce the χ^2 value compared with the 1:1 Langmuir model. The standard deviations of several kinetics constants calculated by complex models were at the same levels as the values of kinetics constants, indicating SPR biosensor could not correctly analyze the detailed kinetics under the present conditions. Therefore the 1:1 Langmuir model was used

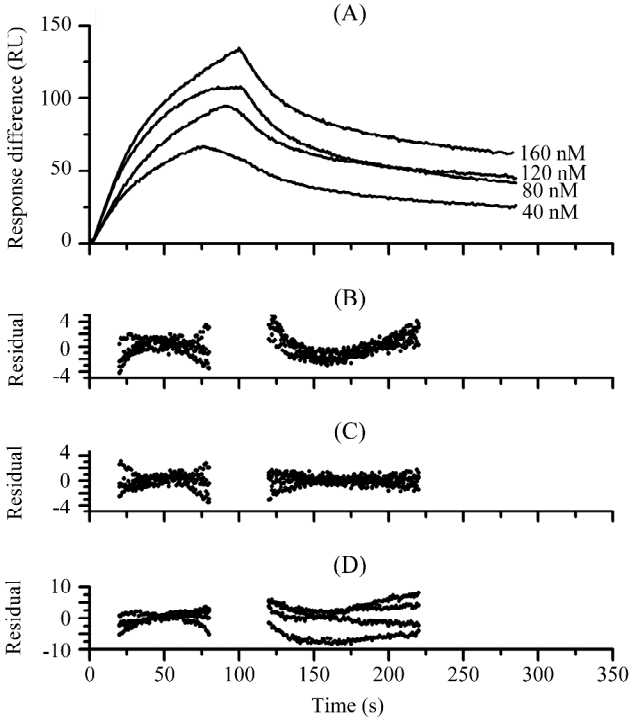

Fig. 3 MMLV RT$^-$ binding responses with the ssDNA and the residual plots for the binding with different models

(A) MMLV RT$^-$ binding responses with the ssDNA, and the residual plots for the binding with the (B) 1:1 Langmuir model, (C) conformation change model and (D) parallel reaction model. The χ^2 values for the three models are 2.64, 0.85 and 12.40, respectively. RU, response unit.

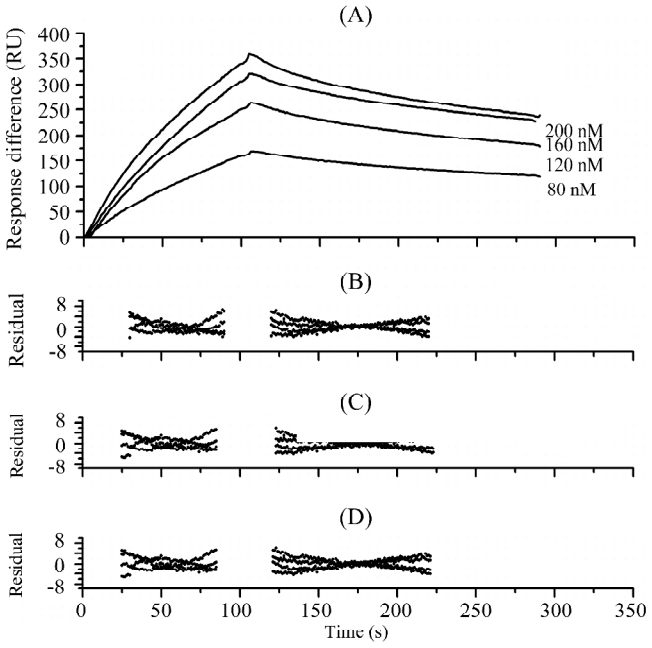

Fig. 4 MMLV RT$^-$ binding responses with the DNA T-P duplex and the residual plots for the binding with different models

(A) MMLV RT$^-$ binding responses with the DNA T-P duplex, and the residual plots for the binding with the (B) 1:1 Langmuir model, (C) conformation change model and (D) parallel reaction model. The χ^2 values for the three models are 4.06, 4.00 and 4.11, respectively. RU, response unit.

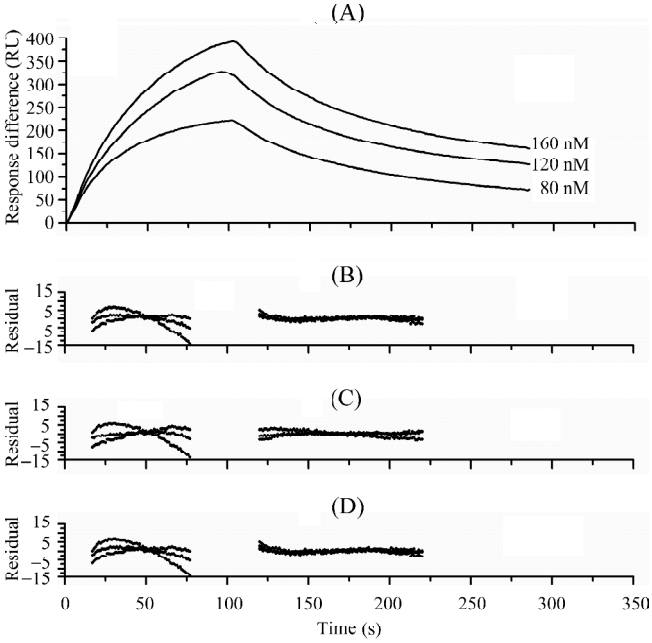

Fig. 5 MMLV RT⁻ binding responses with the gapped DNA and the residual plots for the binding with different models

(A) MMLV RT⁻ binding responses with the gapped DNA, and the residual plots for the binding with the (B) 1:1 Langmuir model, (C) conformation change model and (D) parallel reaction model. The χ^2 values for the three models are 6.63, 6.99 and 6.66, respectively. RU, response unit.

to calculate the kinetics constants and the affinity constants of MMLV RT⁻ binding with the DNA T-P duplex and the gapped DNA (**Table 2**). The affinity of MMLV RT⁻ for the ssDNA (K_A=4.31×10^7 M^{-1}) was 4.5-fold and 9.3-fold higher, respectively, than that of the DNA T-P duplex (K_A=9.64×10^6 M^{-1}) and the gapped DNA (K_A= 4.61×10^6 M^{-1}) (**Table 2**), mostly due to the rapid association and the inclination of transferring to a tight binding conformation. The affinity of MMLV RT⁻ binding with DNA T-P duplex was about twice as high as with the gapped DNA (**Table 2**), which shows the separated components of total response based on the parallel reaction model (**Fig. 6**). Component 1 and component 2 represent two reactions in **Equation (3)**. When RT bound with the gapped DNA, the contribution of component 2 for the binding kinetics was approximately 0, indicating the gapped DNA did not provide the second binding site for RT. MMLV RT⁻ should bind with the T-P part away from the surface of the gapped DNA according to a previous study [15]. However it is possible that there were two different RT binding sites in the DNA T-P duplex. The MMLV RT⁻ bound mostly with the T-P part and the binding with overhang template also affected the total response.

The effects of different inhibitors on the binding interaction between MMLV RT⁻ and the gapped DNA

NNRTIs take effect during DNA polymerization involving RT interaction with T-P. The gapped DNA only provided one RT binding site. MMLV RT⁻ can fully contact with the 15 bp duplex and the 8-mer template overhang [15]. Therefore the gapped DNA was used to study MMLV RT⁻ binding with DNA T-P in the presence of inhibitors. The responses of RT binding with the gapped DNA in the presence of EFV, NVP or quercetin are shown in **Fig. 7**; the residual plots based on the 1:1 Langmuir model showed the binding kinetics were well described by the model. Analysis of the kinetics data demonstrated the discrepancy in the effects of EFV, NVP and quercetin on RT binding with the T-P part of the gapped DNA (**Table 3**). EFV slightly weakened the MMLV RT⁻ binding capability with DNA. The affinity decreased approximately three-fold compared with the affinity measured in the absence of the inhibitor (K_A=1.21×10^6 M^{-1} vs. K_A=4.61×10^6 M^{-1}) due to reduced association. With NVP, MMLV RT⁻ associated with the DNA T-P part quicker and dissociated from DNA slower [k_a=(1.19±0.02)×10^5 M^{-1}·s^{-1} and k_d=(8.1±0.2)×10^{-3} s^{-1}] than without the inhibitor [k_a=(5.11±0.17)×10^4 M^{-1}·s^{-1} and k_d=(1.11±0.02)×10^{-2} s^{-1}] and the total affinity (K_A=1.47×10^7 M^{-1}) increased two-fold. Although quercetin inhibited the activity of both HIV-1 RT and other retrovirus RT in cellular experiments *in vitro* [8,9,19], it hardly interfered the MMLV RT⁻ binding with DNA T-P in

Table 2 Kinetics constants and affinity constants for MMLV RT⁻ binding with different DNA substrates

DNA substrate	k_{a1} (×10^4 M^{-1}·s^{-1})	k_{d1} (×10^{-2} s^{-1})	k_{a2} (×10^{-2} s^{-1})	k_{d2} (×10^{-3} s^{-1})	K_A (×10^6 M^{-1})
ssDNA (conformation change model)	18.50±0.50	2.87±0.21	1.38±0.05	2.41±0.09	43.10
DNA T-P duplex (1:1 Langmuir model)	5.22±0.24	0.54±0.02	NA	NA	9.64
Gapped DNA (1:1 Langmuir model)	5.11±0.17	1.11±0.02	NA	NA	4.61

ssDNA, single-stranded DNA; T-P, template-primer; NA, not available.

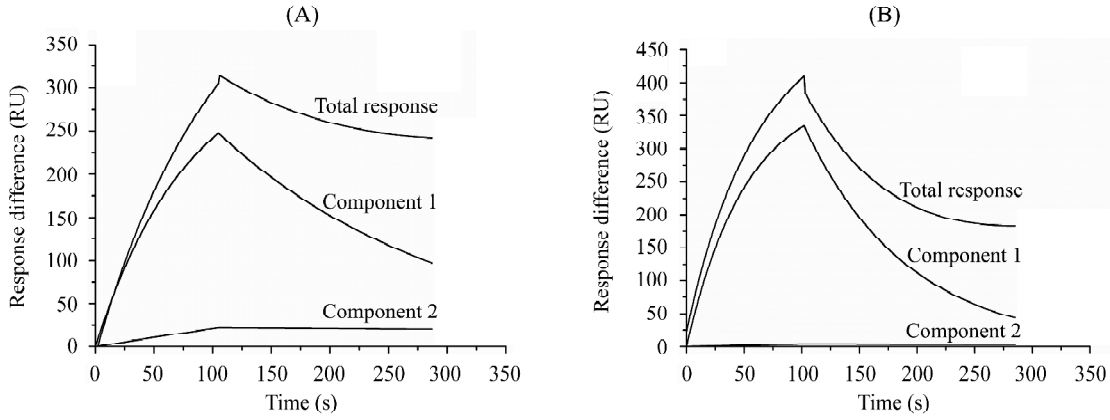

Fig. 6 The two components of the responses of 160 nM MMLV RT⁻ binding with two DNA substrates according to the parallel reaction model

(A) The DNA T-P duplex and (B) the gapped DNA T-P. RU, response unit.

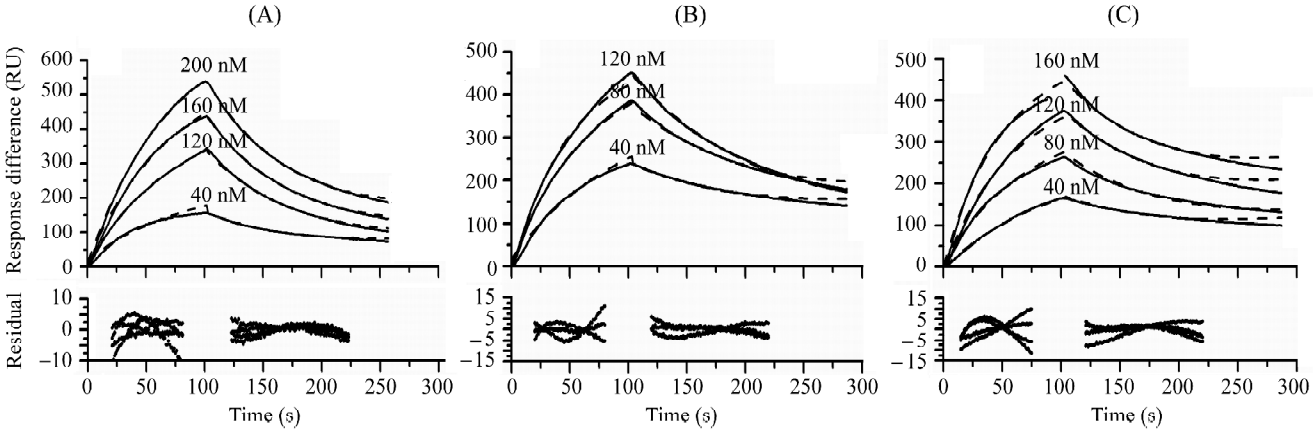

Fig. 7 MMLV RT⁻ binding with the gapped DNA in the presence of different RT inhibitors and corresponding residual plots based on the 1:1 Langmuir model

(A) efavirenz, (B) nevirapine and (C) quercetin. The χ^2 values were 5.23, 6.03, and 10.6, respectively. The solid line represents the actual response curves, the dashed line represents the fitting curves. RU, response unit.

Table 3 Comparison of MMLV RT⁻ binding kinetics with the gapped DNA in the absence and in the presence of inhibitors

1:1 Langmuir model	k_a ($\times10^4$ $M^{-1}\cdot s^{-1}$)	k_d ($\times10^{-2}$ s^{-1})	K_A ($\times10^6$ M^{-1})
MMLV RT⁻ only	5.11±0.17	1.11±0.02	4.61
MMLV RT⁻+EFV	1.55±0.07	1.28±0.01	1.21
MMLV RT⁺+NVP	11.90±0.20	0.81±0.02	14.70
MMLV RT⁻+quercetin	8.56±0.18	1.04±0.02	8.24

EFV, efavirenz; NVP, nevirapine.

our experiments. With quercetin, both the affinity constant, K_A=8.24×10^6 M^{-1}, and the association rate constant, k_a= (8.56±0.18)×10^4 $M^{-1}\cdot s^{-1}$, of MMLV RT⁻ binding with the DNA T-P part of the gapped DNA, increased appreciably.

Discussion

This report demonstrated the use of the SPR biosensor

technique in the characterization of RT binding with different DNA substrates, offering an analytical method for studying the effects of small molecular inhibitors on macrobiomolecule interactions.

Previous studies have suggested that wild HIV-1 RT bound efficiently with the hybrid duplex but relatively weakly with single-stranded RNA. However our results indicated that MMLV RT⁻ bound efficiently with both ssDNA (**Fig. 3**) and DNA T-P (**Figs. 4** and **5**), and RT binding with ssDNA was stronger than that with DNA T-P. The ssDNA used in our experiments did not have a secondary structure at the temperature 25 °C according to the simulation by the minimum free energy algorithm, so MMLV RT⁻ indeed bound with the single-stranded region of DNA. Biochemical studies showed RNase H domain of wild MMLV RT bound with the duplex part of T-P and the MMLV RT⁻ without RNase H domain could not stably bind with T-P [15,20], which shows that MMLV RT⁻ has low affinity with T-P duplex.

The SPR biosensor technique can resolve complex mechanisms of biomolecular interactions [11,21,22]. Effective use of a complex model to interpret SPR data depends on many factors, such as quality of fit, structures and properties of the components being studied, and comparison with results obtained by other techniques. In order to minimize the deviation from true kinetics parameters, all kinetic analyses were performed by global fitting. RT binding with DNA is a complex kinetic process with initial collision of the enzyme and DNA followed by conformation change based on the pre-steady kinetics study [4,18]. However, the conformation change model could not satisfactorily analyze RT binding with the DNA T-P duplex or the gapped DNA immobilized on the biosensor surface in our experiments because of the large standard deviation of kinetics constants. Similarly, the parallel reaction model was inadequate for the calculation of kinetics parameters although there might be two different RT binding sites in the DNA T-P duplex or the gapped DNA according to the length and components of DNA [15]. **Fig. 6** illustrates that RT binding with the second site was weak or even negligible. The 75 kDa RT bound with the T-P part away from the surface, which significantly interfered with the contact of the enzyme with the DNA part in the vicinity of the surface. Because of strong binding capability with the ssDNA, a small number of MMLV RT⁻ bound with the ssDNA part of the DNA T-P duplex and slightly enhanced the total affinity of the binding. The overall reaction fitted well with the 1:1 Langmuir model, which could be used to describe properties of the overall binding due to the predominance of rate-limiting association and dissociation steps.

Both EFV and NVP are non-nucleotide drugs against HIV-1 RT as approved by the USA's Food and Drug Administration. Quercetin, a flavonoid of plant origin, was found to almost completely inhibit MMLV RT and HIV-1 RT [9,19]. Using the SPR biosensor technique, we estimated the effects of these inhibitors on RT binding with DNA by comparing their kinetics parameters. The 1:1 Langmuir model well described the binding and was used to analyze the binding kinetics. In our experiments, the binding activity of MMLV RT⁻ with T-P was slightly reduced in the presence of EFV. RT bound with T-P more tightly in the presence of NVP than in its absence. Quercetin had a small effect on the kinetics of RT-DNA binding and the total affinity slightly increased. Previous kinetics experiments suggested that the inhibition of RT induced by NNRTIs was achieved mainly through blocking the chemical step of DNA synthesis by forming a closure and non-productive ternary complex [4,23]. A slight decrease in affinity of RT-EFV with T-P can be explained by the mixed non-competitive inhibiting model [6]. The binding affinity of RT with T-P duplex increased with the presence of NNRTIs, for example, the affinity of the T-P duplex was increased by at least a factor of 10 in the presence of O-TIBO [4]. Our results confirmed that NNRTIs, such as EFV or NVP, had a small inhibition or no inhibition during RT binding with T-P. The relatively tight binding of RT with DNA in the presence of NVP indicated the inhibitor might deform the natural structure of the DNA binding site in RT by the communication between the inhibitor binding site and the active site in RT. Previous studies showed that NVP and EFV could enhance HIV-1 RT dimerization [24–27] and the binding of NNRTI caused a decrease in the flexibility in the subdomain of RT [25,26, 28–30]. Nevertheless, how these conformation changes interfere with RT action on nucleotide acid substrates needs further study. Quercetin is not an analog of nucleotide or nucleoside and has poor solubility in water. Our data suggested this natural compound did not interfere with RT binding with DNA T-P. Three possibilities exist for the inhibiting mechanism of quercetin. First, quercetin might act like an NNRTI. Second, quercetin may interfere with chemical reaction steps during RT-mediated DNA synthesizing. Finally, published structural information on the inhibition of phosphoinositide 3-kinase by flavones suggest quercetin is located in the ATP binding pocket of phosphoinositide 3-kinase [31]. We presumed there existed a similar mode during the interaction between quercetin and RT. On the other hand, some studies suggest quercetin is also the inhibitor of integrase [9,32], pol β and pol I [8],

so quercetin might interact with other biomolecules before contacting with RT.

References

1 Arnold Eicalournal, Georgiadis MM, Jessen SM, Ogata CM, Telesnitsky A, Goff SP, Hendrickson WA. Mechanistic implications from the structure of a catalytic fragment of moloney murine leukemia virus reverse transcriptase. Structure 1995, 3: 879–892

2 Motakis D, Parniak MA. A tight-binding mode of inhibition is essential for anti-human immunodeficiency virus type 1 virucidal activity of nonnucleoside reverse transcriptase inhibitors. Antimicrob Agents Chemother 2002, 46: 1851–1856

3 Rittinger K, Divita G, Goody RS. Human immunodeficiency virus reverse transcriptase substrate-induced conformational changes and the mechanism of inhibition by nonnucleoside inhibitors. Proc Natl Acad Sci USA 1995, 92: 8046–8049

4 Huang H, Chopra R, Verdine GL, Harrison SC. Structure of a covalently trapped catalytic complex of HIV-1 reverse transcriptase: Implications for drug resistance. Science 1998, 282: 1669–1675

5 Maga G, Ubiali D, Salvetti R, Pregnolato M, Spadari S. Selective interaction of the human immunodeficiency virus type 1 reverse transcriptase nonnucleoside inhibitor efavirenz and its thio-substituted analog with different enzyme-substrate complexes. Antimicrob Agents Chemother 2000, 44: 1186–1194

6 Yang SS, Cragg GM, Newman DJ, Bader JP. Natural product-based anti-HIV drug discovery and development facilitated by the NCI developmental therapeutics program. J Nat Prod 2001, 64: 265–277

7 Ono K, Nakane H, Fukushima M, Chermann JC, Barre-Sinoussi F. Differential inhibitory effects of various flavonoids on the activities of reverse transcriptase and cellular DNA and RNA polymerases. Eur J Biochem 1991, 190: 469–476

8 Tewtrakul S, Nakamura N, Hattori M, Fujiwara T, Supavita T. Flavanone and flavonol glycosides from the leaves of *Thevetia peruviana* and their HIV-1 reverse transcriptase and HIV-1 integrase inhibitory activities. Chem Pharm Bull 2002, 50: 630–635

9 Middleton E Jr, Kandaswami C, Theoharides TC. The effects of plant flavonoids on mammalian cells: Implications for inflammation, heart disease and cancer. Pharmacol Rev 2000, 52: 673–751

10 Tsoi PY, Yang M. Surface plasmon resonance study of the molecular recognition between polymerase and DNA containing various mismatches and conformational changes of DNA-protein complexes. Biosens Bioelectron 2004, 19: 1209–1218

11 Tsoi PY, Yang J, Sun YT, Sui SF, Yang MS. Surface plasmon resonance study of DNA polymerases binding to template/primer DNA duplexes immobilized on supported lipid monolayers. Langmuir 2000, 16: 6590–6596

12 Gorshkova II, Rausch JW, le Grice SF, Crouch RJ. HIV-1 reverse transcriptase interaction with model RNA-DNA duplexes. Anal Biochem 2001, 291: 198–206

13 Linnell J, Mott R, Field S, Kwiatkowski DP, Ragoussis J, Udalova IA. Quantitative high-throughput analysis of transcription factor binding specificities. Nucleic Acids Res 2004, 32: e44

14 Wohrl BM, Georgiadis MM, Telesnitsky A, Hendrickson WA, le Grice SF. Footprint analysis of replicating murine leukemia virus reverse transcriptase. Science 1995, 267: 96–99

15 Sjolander S, Urbaniczky C. Integrated fluid handling system for biomolecular interaction analysis. Anal Chem 1991, 63: 2338–2345

16 Luo J, Zhou J, Zou W, Shen P. Antibody-antigen interactions measured by surface plasmon resonance: Global fitting of numerical integration algorithms. J Biochem 2001, 130: 553–559

17 Wohrl BM, Krebs R, Goody RS, Restle T. Refined model for primer/template binding by HIV-1 reverse transcriptase: Pre-steady-state kinetic analyses of primer/template binding and nucleotide incorporation events distinguish between different binding modes depending on the nature of the nucleic acid substrate. J Mol Biol 1999, 292: 333–344

18 Farmerie WG, Loeb DD, Casavant NC, Hutchison CA 3rd, Edgell MH, Swanstrom R. Expression and processing of the AIDS virus reverse transcriptase in *E. coli*. Science 1987, 236: 305–308

19 Telesnitsky A, Goff SP. RNase H domain mutations affect the interaction between Moloney murine leukemia virus reverse transcriptase and its primer-template. Proc Natl Acad Sci USA 1993, 90: 1276–1280

20 Tsoi PY, Yang MS. Kinetic study of various binding modes between human DNA polymerase β and different DNA substrates by surface-plasmon-resonance biosensor. Biochem J 2002, 361: 317–325

21 Lipschultz CA, Li Y, Smith-Gill S. Experimental design for analysis of complex kinetics using surface plasmon resonance. Methods 2000, 20: 310–318

22 Spence RA, Kati WM, Anderson KS, Johnson KA. Mechanism of inhibition of HIV-1 reverse transcriptase by nonnucleoside inhibitors. Science 1995, 267: 988–993

23 Sluis-Cremer N, Tachedjian G. Modulation of the oligomeric structures of HIV-1 retroviral enzymes by synthetic peptides and small molecules. Eur J Biochem 2002, 269: 5103–5111

24 Tachedjian G, Goff SP. The effect of NNRTIs on HIV reverse transcriptase dimerization. Curr Opin Investig Drugs 2003, 4: 966–973

25 Tachedjian G, Aronson HE, de los Santos M, Seehra J, McCoy JM, Goff SP. Role of residues in the tryptophan repeat motif for HIV-1 reverse transcriptase dimerization. J Mol Biol 2003, 326: 381–396

26 Tachedjian G, Orlova M, Sarafianos SG, Arnold E, Goff SP. From the Cover: Nonnucleoside reverse transcriptase inhibitors are chemical enhancers of dimerization of the HIV type 1 reverse transcriptase. Proc Natl Acad Sci USA 2001, 98: 7188–7193

27 Kohlstaedt LA, Wang J, Friedman JM, Rice PA, Steitz TA. Crystal structure at 3.5 Å resolution of HIV-1 reverse transcriptase complexed with an inhibitor. Science 1992, 256: 1783–1790

28 Pauwels R, Peletskaya EN, Kogon AA, Tuske S, Arnold E, Hughes SH. Nonnucleoside inhibitor binding affects the interactions of the fingers subdomain of human immunodeficiency virus type 1 reverse transcriptase with DNA. J Virol 2004, 78: 3387–3397

29 Mizushina Y, Iida A, Ohta K, Sugawara F, Sakaguchi K. Novel triterpenoids inhibit both DNA polymerase and DNA topoisomerase. Biochem J 2000, 350: 757–763

30 Kim HJ Woo ER, Shin CG, Park H. A new flavonol glycoside gallate ester from *Acer okamotoanum* and its inhibitory activity against human immunodeficiency virus-1 (HIV-1) integrase. J Nat Prod 1998, 61: 145–148

Edited by
Ping WANG